17th World Conference on Earthquake Engineering, 17WCEE
Sendai, Japan - September 13th to 18th 2020

SEISMIC CRACKING DAMAGE ANALYSIS FOR THE PC GIRDERS OF MIAOZIPING BRIDGE DURING 2008 WENCHEN EARTHQUAKE

D.S. Wang[1], L. Tong[2]

[1] *Professor, School of Civil and Transportation Engineering, Hebei University of Technology, Tianjin, P.R. China, e-mail: dswang@hebut.edu.cn*
[2] *PhD student, School of Civil and Transportation Engineering, Hebei University of Technology, Tianjin, P.R. China, e-mail: leitong185@163.com*

Abstract

The box girder of Miaoziping Bridge, a three-span frame bridge, cracked seriously and had a large lateral residual displacement at the end of box in Wenchuan earthquake. In order to further understand the damage causes of main girder cracking, eight strong motion records near the bridge site and the general used El Centro and Taft records are selected as the inputs for time history analysis the bridge. The cantilever construction process and initial stress of the box girder are considered in bridge model for seismic numerical simulation. In addition, numerical simulation results are compared with the actual earthquake damage. The results show that the high stress zones of the box girder are agreed with the seismic damage when various seismic inputs are considered, which indicate that the cracking damage of the box girder is not an individual phenomenon. In strong earthquake, it is prone to reach high tensile stress state and high compressive stress state in some zones, such as the top plate near the main pier and the closure sections of the side span and the middle span, and the web near 1/6 to 1/2 side span and the middle span of 1/4 to 3/4, and the bottom plate near the closure section and the adjacent 2-3 sections of the side span and the middle span. Under the seismic input of Mianzhu and Qingping record in Wenchuan earthquake, they are far beyond the limited tensile stress of concrete for the maximum (principle) tensile stress in top plate and web of the side span and the middle span. Similarity the tensile stress of the bottom plate is close to the limited tensile stress of concrete near the middle span. Under the seismic actions, the estimated stress of the longitudinal prestressed tendons increase to nearly 100 MPa.

Keywords: Wenchuan earthquake, Miaoziping Bridge, earthquake damage analysis; box girder cracking

1. Introduction

In the western regions of China with high seismic risks, many continuous rigid frame bridges with high piers and long spans were constructed in the last two decades. At present, a lot of researches have been carried out on the seismic performance of the long-span rigid frame bridges with high piers. In addition to the discussion of the seismic ductility [1], They also involve the hydrodynamic impact and seismic vulnerability [2,3], topography effects and multi-dimensional earthquake excitations [4,5,6,7]. Yan [8]and Zong [9] also carried out shaking table tests on seismic responses for rigid frame bridges with scale ratio of 1:10 and 1:15 respectively. In these studies, it is generally believed that the earthquake damage will be concentrated on the bridge piers, and the main girder will keep elastic during earthquake. According to the bridge seismic design code JTG/T B02-01-2008 in China [10], only the pier is designed considering its ductility under the seismic actions, for the supper structure of the bridge is generally designed by the combinations of the dead load, live load and temperature load, et al. The seismic performance of the girder is not described in detail and is considered it will be elastic.

For the multi-span rigid frame bridge with high pier and long span, although piers have a certain flexibility, it still has the same mechanical properties as the rigid frame, when the horizontal force is applied to the frame, the beam will have resisting forces. Because the main girder and the pier are rigid together in the frame bridge, instead of the bearings are used between them like the simply supported bridge or the continuous bridge do. The girder will certainly resistant the seismic force together with the pier, especially for the earthquake input in longitudinal and vertical directions of the bridge. If the ground motions get more larger, the main girder with prestressed reinforced concrete (PRC) may crack in the strong earthquake.

The 2008 Ms8.0 Wenchuan earthquake resulted in obvious damages of Miaoziping Bridge, which is located less than 15km from the earthquake epicenter. The main bridge and the approach bridge were both damaged. The girder had been falling down in the 10th span for the approach bridge which is simply supported. And the cracking was at the foot of the No.5 main pier under the water for the main bridge which is a rigid frame bridge. It was worth noting that the box girder of main bridge had a very serious cracking phenomenon, the side span had a large residual displacement as well. These damages were hardly seen in previous bridge damage in earthquakes [11,12]. It is also the first domestic case of earthquake damage of a large-span continuous rigid frame bridge with above 100-meter-high piers in recent years, which deserves to pay more attention to the damage mechanism.

Before the Wenchuan earthquake, the seismic performance had been evaluated by Xia [13] assuming that the potential earthquake of Ms 7.0 would occur for design. It can be ensured that the pier will not be damaged and the plastic hinge will not be produced during the considered design earthquake. Yao [14] also proposed the seismic design method of the bridge, the seismic forces were considered for the substructure (e.g. piers) according to the peak ground motion of acceleration (PGA) with 0.24g, with the probability of exceedance of 2% in 100 years.

After the 2008 Wenchuan earthquake some field investigations and research were carried out for the Miaoziping Bridge. Wang [15,16] pointed out that the main bridge could meet the seismic design objectives, which had not collapse under the large and strong earthquake, but more attention should be paid to the seismic damage and control for such multi-span rigid frame bridges. Shan [17,18] analyzed the seismic vulnerability and the influence of fault distances on the main bridge. Deng [19] discussed the Water-pier coupling effect of the main bridge and the impact of the longitudinal collision of the girders on the piers.

All of the researches focus on the response of piers of the Miaoziping Bridge, only Yang [20] made a discussion on the seismic damage of the main girders of Miaoziping bridge. it was considered that the tensile stress at the bottom plate of the box girder exceed the tensile strength of the concrete in the closure section of the side span of the bridge during the earthquake. It was found that the alternating stress of tension and compress would cause the cracking of the main girder easily.

Generally speaking, for Miaoziping Bridge there is still a lack of comparative analysis of the cracking of the girder to the real seismic damage by numerical simulation, and the analysis of the cracking mechanism should be revealed. Based on the actual seismic damage of the box girder of Miaoziping Bridge in 2008 Wenchuan Earthquake, the initial stress along the section of the box girder is obtained by considering the construction process with the model developed by Midas software, then the time history analysis with the records during the earthquake is carried out. The cracking mechanism of the box girder is discussed by the maximum tensile or compressive stress of the girder's section under the seismic action. The tensile stress changing of the prestressed reinforcement is also given.

2. Miaoziping Bridge and Finite Element Model

The Miaoziping bridge is located 15km upstream of the dam of Zipingpu Reservoir in Dujiangyan, Sichuan Province. The main bridge is a prestressed concrete continuous rigid frame bridge with spans of 125m+220m+125m. The main bridge girder was designed by three dimensional prestressed systems with single-box and single-chamber section (Fig.1). The box girder was designed according to a full-prestressed structure which means that the tensile stress was not allowed for the bridge operation. No.4 pier and No.5 pier both adopted a rectangular hollow section, and No.3 pier and No.6 pier adopted a double-column thin-wall hollow section. Pile group foundations were taken and supported by the stratum or bedrock. The girder was made of C60 concrete while the pier was made of C40 concrete. The two-way movable basin rubber bearings were installed on the top of the piers on each side-span of the bridge, their vertical bearing capacity of 10MN, the allowable maximum longitudinal displacement of 20cm, the allowable maximum lateral displacement of 4cm.

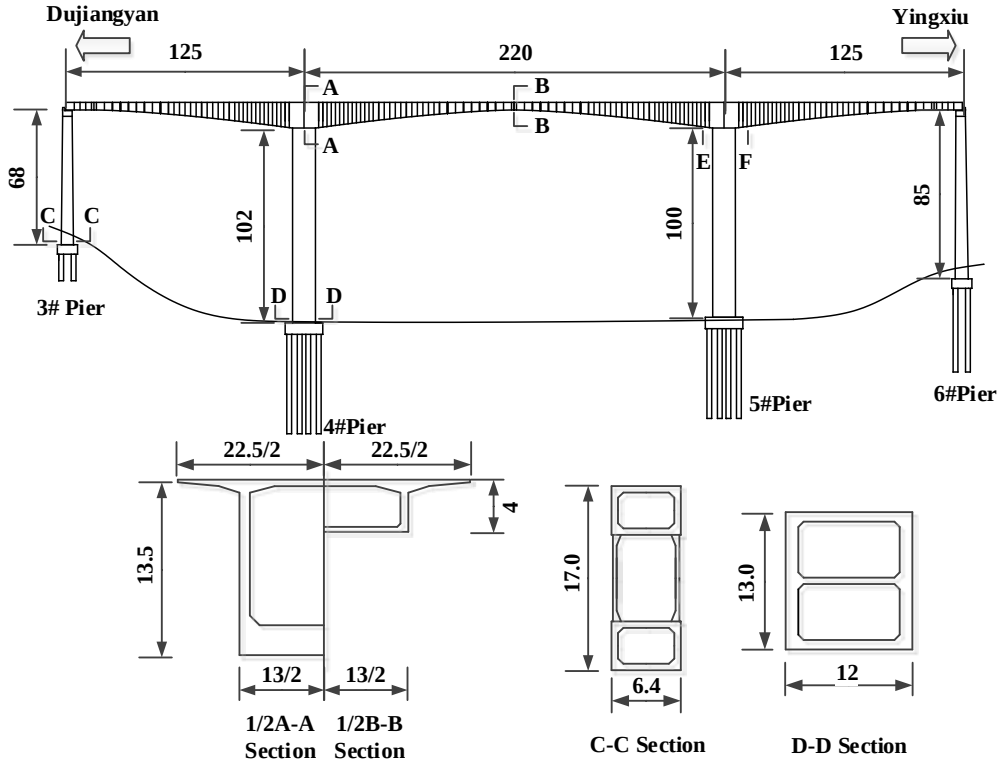

Fig. 1 – Arrangement of Bridge Span and Cross Section （unit: m）

Seismic design of the bridge was based on the site's seismic intensity of VII degrees with the PGA equaling to 0.1g, and the seismic performance was evaluated with a PGA of 0.24g, with the probability of exceedance of 2% in 100 years. When the Wenchuan earthquake occurred, the main bridge of Miaoziping bridge had just completed construction, only the expansion joints had not been installed, and the main girder

had no initial damage and cracking. It had been reported that, in the long-term service of the rigid frame bridge, there were common engineering problems such as midspan deflection, web cracking and prestress loss of the main girders [21,22].

Finite element modeling is performed using Midas Civil software and the main girder is set with 162 beam elements. Because the pile foundations enter the rock layer to a certain depth and the cover layer thickness is 10m, soil-structure interaction is not considered. The half-span loads of adjacent approach bridges are simplified as the concentrated mass, which is applied on the top of each side span pier.

The main bridge was constructed by cantilever cast method at the site. At first step, according to the construction process the initial stress under the dead load for the section of the girder is present. The numerical simulation for construction process includes applying hanging basket, wet weight acting, deck pavement loading, and prestressed loading with 402 pre-stressing tendons (Fig.2). The bearings are simulated by setting the elastic connection. Because the spacing between the main girder and the shear keys is only 10cm (including 7cm thick rubber block) in the transverse direction of the bridge, so the transverse displacement between the girder and the pier is constrained. In addition, constraint in the longitudinal direction of the bridge is released (Fig.3).

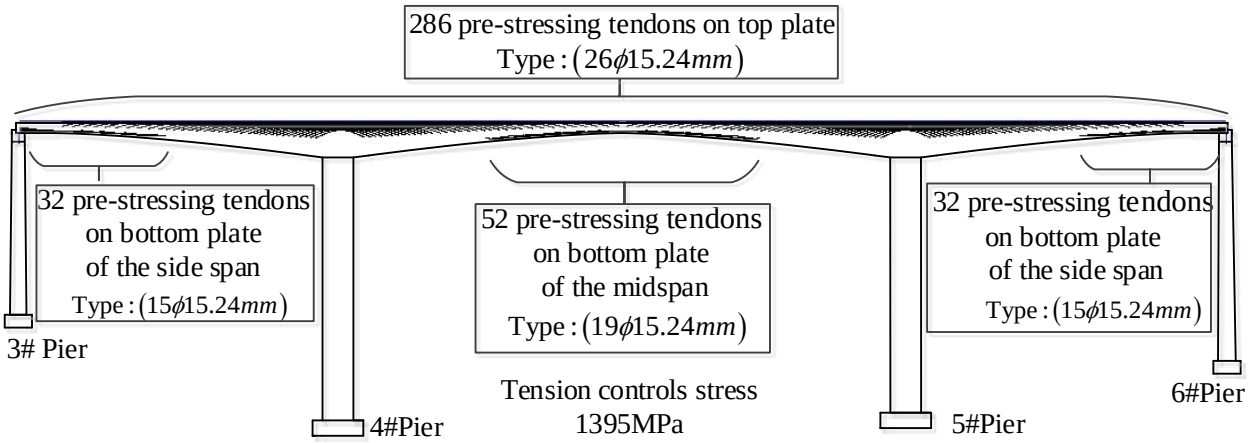

Fig. 2 –Pre-stressing Tendons in the Model

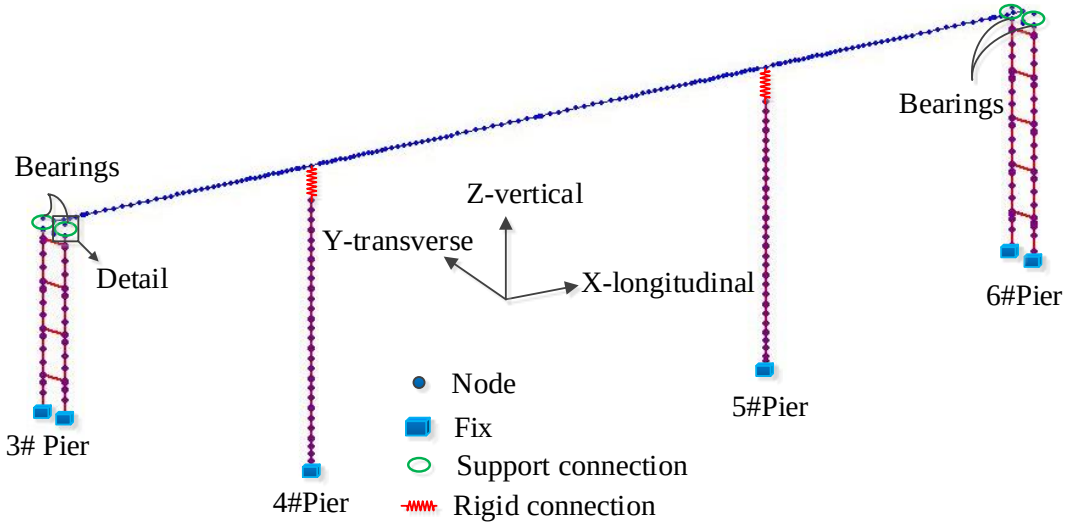

(a) Finite Element Modeling

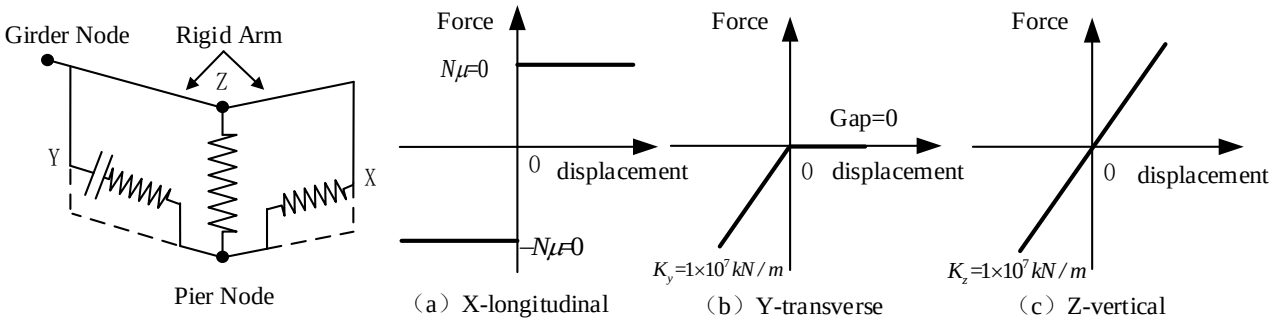

(b) The Detail of Boundary Conditions of Side Span Piers

Fig. 3 –Modeling and Boundary Conditions of Bridge

E point and F point were stress monitoring points for the main girder during the bridge construction at the site (see Fig.1). These points were also at the top of the No.5 pier under the cantilever construction process for the bridge. Ma [23] carried out the on-site construction monitoring of the main bridge, and obtained the value of the bottom plate stress of point E and point F of the min girder. Fig.4 shows the comparison between the simulation results of this paper and the field measurement results of Ma's. It can be seen that the simulation results are in good agreement with the measured stress trends. The results in this paper are minor small during the cantilever pouring process, but the final stress is less than 1MPa from the actual monitoring data. This proves that the theoretical calculations are basically in line with the actual construction process, and verifies the accuracy of the initial stress of the main girder of the bridge.

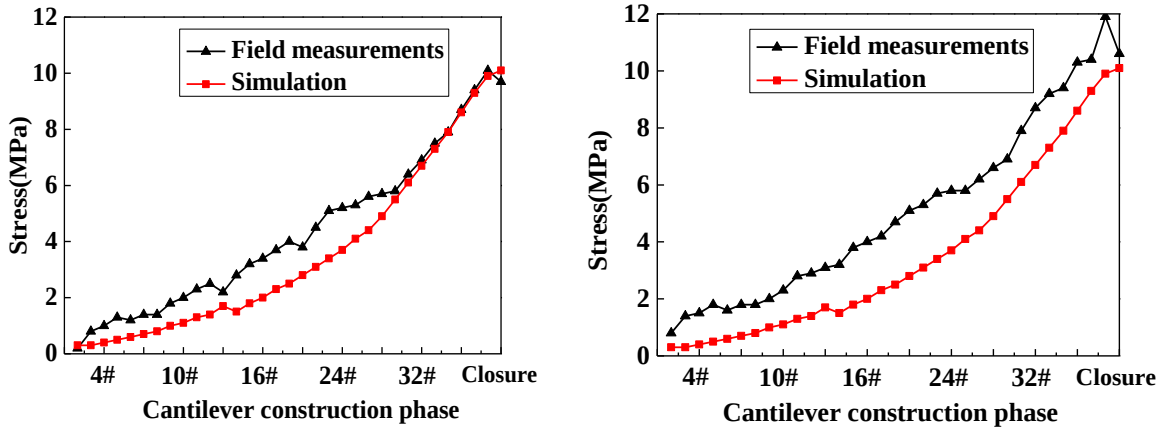

(a) The Stress of E Point (b) The Stress of F Point

Fig. 4 – Comparison of Simulation and Actual Measured Stress

The initial (principle) tensile stress and compressive stress of the top plate, bottom plate and web of the box section of the girder after completion of the bridge are shown in Fig.5. The stress for web is taken from the point where chamfer of the web plate and the bottom plate are intersected. It can be seen that all the sections of box girder are basically in full compression state. In addition, there are large peak values at the girder's sections near the piers, they are may be influenced by the piers, so the stress calculation values at these positions are only for reference, the same below.

The vibration modes of the main bridge are analyzed and show that the five of the first ten modes are mainly dominated by the transverse vibration of the main girder. The first vibration mode is symmetric lateral displacements of the main girder and the pier with the frequency of 0.32Hz. Guo [24] had test the dynamic characteristics of the main bridge on site after the Wenchuan earthquake. Table.1 shows the comparison between the calculation results in this paper and the test results. It can be seen that the errors of the natural frequencies are less than 6%.

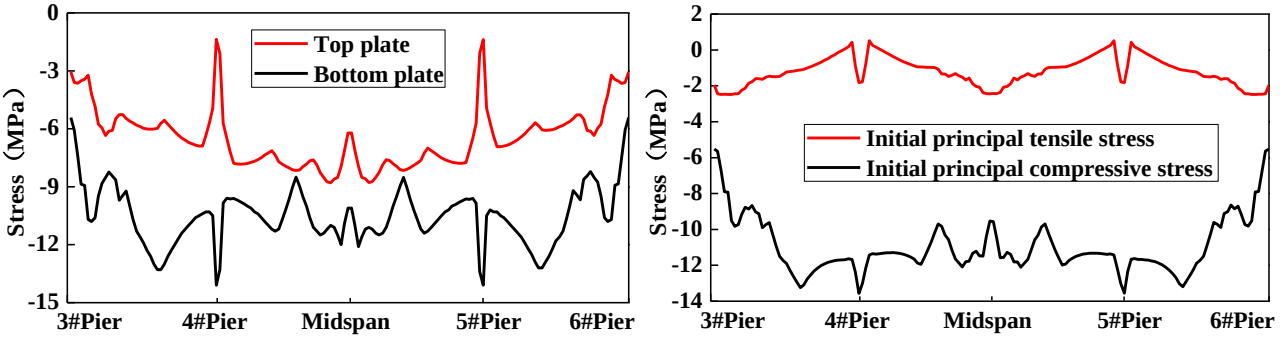

(a) Top Plate and Bottom Plate (b) Web of Box Girder

Fig. 5 – Initial Stress of Box Girder Section

Table 1 – Comparison of Simulation and Actual Measured Frequency

Vibration shape	method	frequency (Hz)	eeror(%)
transverse vibration of girder	field measurements	0.31	3%
	Simulation	0.32	
vertical vibration of mid-span	field measurements	0.93	-6%
	Simulation	0.87	

3. Earthquake Records Selection

The bridge site, earthquake faults and record stations are shown in Fig. 6, and the information of eight stations near the bridge site is shown in Table 2. It can be seen that the bridge site is located between the two faults, and the distance from the Beichuan-Yingxiu fault is less than 6km. The longitudinal direction of the bridge is 50 °to the north by west, and the intersection angle with the Beichuan-Yingxiu fault is about 40 °. The peak values of ground accelerations (PGAs)of the stations near the fault, such as Wenchuan Wolong (051WCW) station, Mianzhu Qingping (051MZQ) station and Shifang Bajiao station (051SFB), are relatively large. MZQ station which close to the fault surface rupture is located between the two faults as same as the bridge does. Fig. 7 shows the earthquake record of MZQ station.

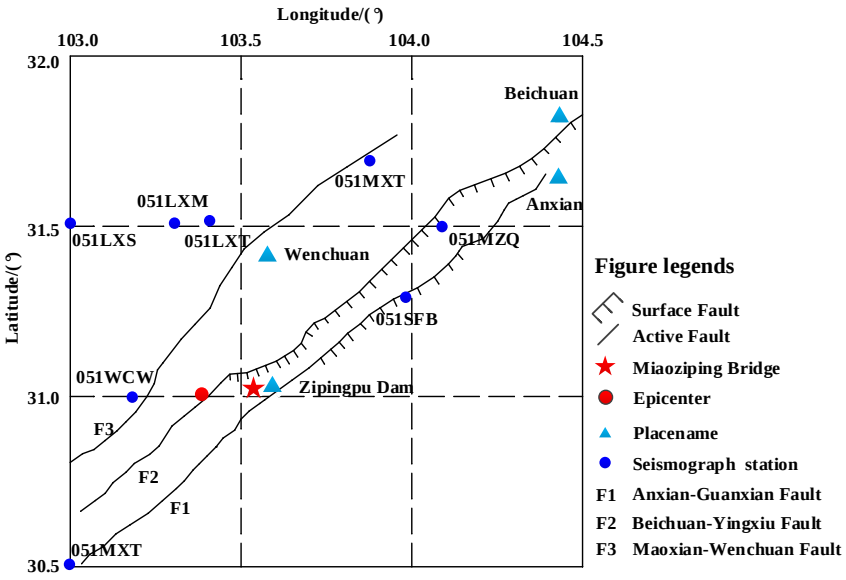

Fig. 6 –Bridge, Fault and Earthquake Record Station

Table.2 –Information of Earthquake Record Station

Station NO.	Name	Site classification	PGA(g)		
			EW	NS	UP
051WCW	Wenchuan Wolong	II	0.957	0.652	0.948
051SFB	Shifang Bajiao	II	0.556	0.581	0.633
051MZQ	Mianzhu Qingping	II	0.824	0.802	0.622
051MXT	Maoxian Diban	bedrock	0.306	0.302	0.266
051LXT	Lixian Taoping	II	0.339	0.342	0.379
051LXM	Lixian Muka	II	0.32	0.283	0.357
051LXS	Lixian Shaba	ground soil	0.221	0.261	0.211
051BXZ	Baoxing Mingzhi	ground soil	0.153	0.117	0.109

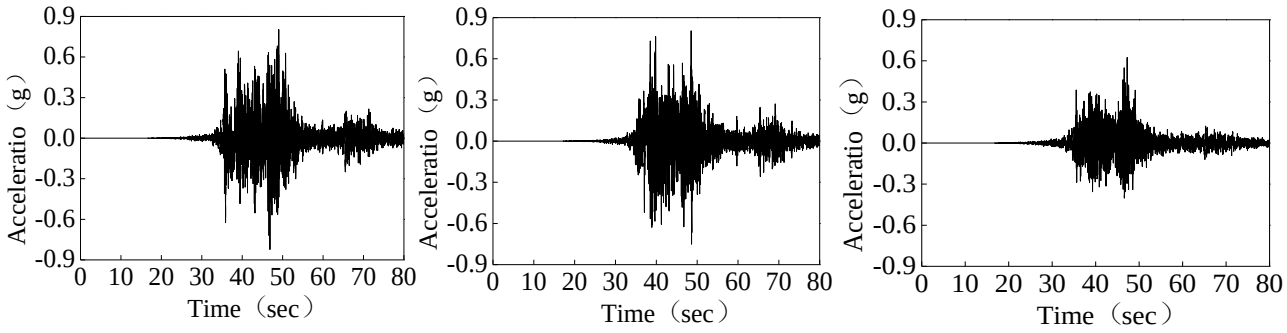

（a）EW （b）NS （c）UP

Fig. 7 – Earthquake Record of Mianzhu Qingping Station

The 8 groups of earthquake records in Table 2 together with the commonly used El Centro and Taft records, total10 groups of records are used in the time history analysis of the bridge. records are divided into two groups, one group is the original seismic waves without amplitude modification, the other group the records' PGAs are adjusted to 0.55g, 0.55g and 0.37g for NS, EW and vertical components respectively，as the same as the seismic damage analysis of Zipingpu Dam analysis by Kong [25]. Kong [25] demonstrated that the records of the Maoxian Diban(051MXT) after amplitude scaling could be used as the ground motion input for the Zipingpu Dam (about 2.9km from the bridge site) in the Wenchuan earthquake.

Considering the longitudinal direction of the bridge is 50° to the north by west, coordinate rotation is carried out for two horizontal ground motion accelerations of EW and NS components, as shown in Eq. (1).

$$\begin{aligned} X_{/\!/} &= X_{EW} \cdot sin(\theta) + X_{NS} \cdot cos(\theta) \\ X_{\perp} &= X_{EW} \cdot cos(\theta) - X_{NS} \cdot sin(\theta) \end{aligned} \tag{1}$$

where, θ is the angle between the longitudinal direction of the bridge and EW direction, taking 50 °; $X_{/\!/}$ and $Y_{\perp}$ are the horizontal components of ground motions for longitudinal direction and transverse direction of the bridge.

4. Main girder Cracking Damage and Numerical Simulation

Time history analysis for the bridge is carried out considering the initial internal force of the dead load under the 10 groups of ground motions. Due to the limited length of the paper, only the stress responses of

the main girder under the ground motions with the scaled amplitude are given. The difference between the actual seismic damage and stress under El Centro ground motion is large, omitted.

The comparison between the actual seismic damage of the main girder and the simulation results is shown in Fig. 8, Fig. 9 and Fig. 10. For the web of the girder's section, the solid lines represent the maximum (principle) tensile stress, the dotted lines represent the maximum (principle) compressive stress; and the thickened real lines and dotted lines represent the records with larger stress responses.

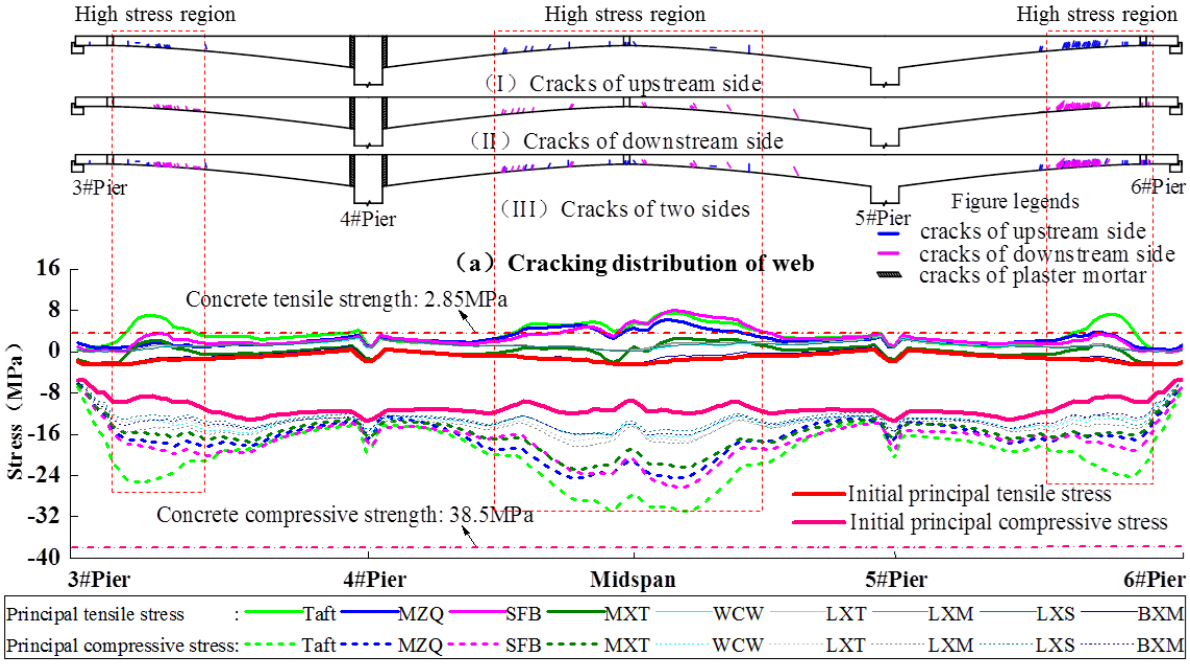

Fig. 8 – Comparison of the Seismic Damage and Numerical Simulation of the Web

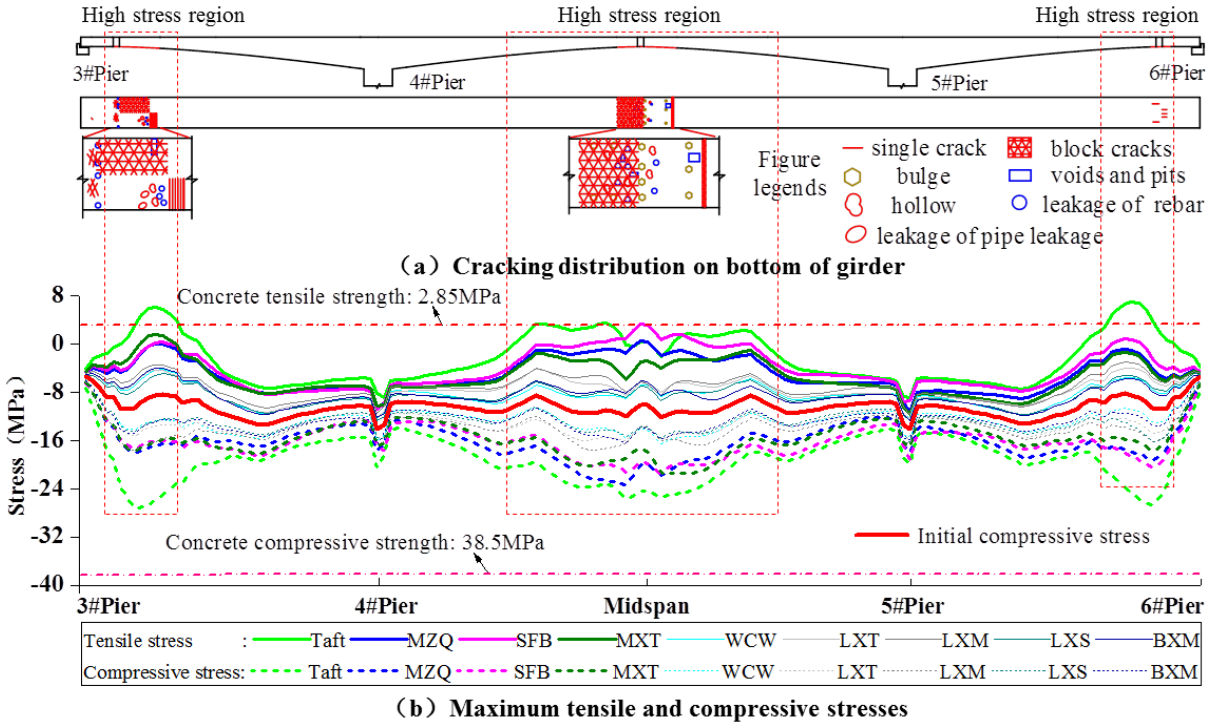

Fig. 9 – Comparison of Seismic Damage and Numerical Simulation of the Bottom Plate

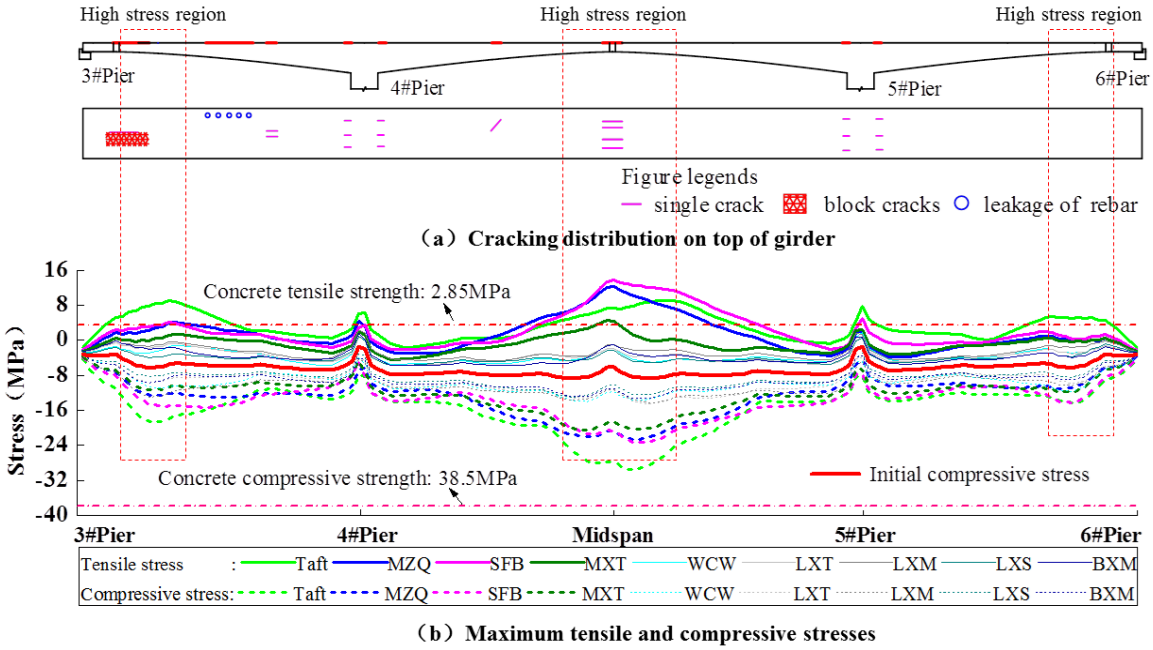

Fig. 10 – Comparison of the Seismic Damage and Numerical Simulation of the Top Plate

Generally speaking, the stress response trends of different records are almost the same, but the magnitudes are different. The stress responses of 051LXT, 051LXM, 051LXS, 051MXM and 051WCW have relatively small values which are not in accordance with the actual earthquake damage of the bridge. Under the input of 051MZQ, 051SFB and 051MXT, the values of the stress are in good agreement with the earthquake damage of the girder. Based on the spatial location of record stations, bridge site and faults, the stress responses of the main girder are discussed by taking the ground motion of 051MZQ as the example in the follow.

The cracks in the web of the girder' section were mainly inclined cracks, which develop from the bottom to the top of the section. The distributions of cracks along the bridge in the upstream and downstream are nearly the same, mainly located in the areas of 1/6-1/2 side span length and 1/4-3/4 middle span length. The cracking damage areas are highly consistent with the maximum tensile zones and compressive stress zones obtained by the numerical simulation. For middle span, the principle tensile stress of the web, at the girder's section 15m away from the closure section of the middle span (close to the side of No.5 pier), is 8MPa. The value far exceeds the standard value of the axial tensile strength of C60 concrete (2.85MPa), and The main compressive stress is 24MPa, which is close to the standard value of the axial compressive strength of C60 concrete (38.5MPa). For two side spans, the principle tensile and principle compressive stress of the webs are not relatively large, the maximum principle tensile stress reaches 3.5MPa, and the maximum principle compressive stress reaches 17MPa.

Cracks for the bottom plate of the section are mainly concentrated in the closure section for construction process during Wenchuan earthquake, either in the mid-span or in the side span of the bridge, as well as 2 to 3 adjacent sections of the closure section. For closure sections, the concretes in the mid-span and side span appear failure in local part of the underneath of the girder, and there are traces of extrusion and spalling of the concrete. Generally, the actual crack zones are closer to the high tensile stress distributed areas and high compressive stress distributed areas, which are obtained by numerical simulation. The numerical simulation shows that the tensile stress of the bottom plate reaches 2MPa in the mid-span, which is close to the standard value of concrete tensile stress. The compressive stress increases by 15MPa compared to the initial stress, reaching 24MPa, which is close to the standard value of concrete compressive strength. The tensile stress and compressive stress of side span are relatively small, the maximum tensile stress is less than 1MPa, and the maximum compressive stress increases about 9MPa compared with the initial stress, reaching 17MPa.

Seismic damage of the inner top plate of the box girder section showed that the distribution of the cracks was regular. Cracks mainly appeared at the junction of the pier and the girder and near the closure sections of the side span and the mid-span. The earthquake damage on the outer top plate could not be observed because of the road pavement completing. The numerical simulation results are also consistent with the earthquake damage of the main girder, but the numerical results discover that the earthquake damage on the outer surface is greater than that on the inter surface for the top plate of the box section. The tensile stress and compressive stress of the top plate at 1/3 of the side span length and at the mid-span are higher than other areas. The maximum tensile stress in the mid-span increases nearly 17MPa compared with the initial stress(-6Mpa), reaching to 12MPa, which far exceed the standard value of the axial tensile strength of the C60 concrete; the compressive stress reaches 23MPa, increasing 18MPa compared with the initial stress(5MPa). The tensile stress and compressive stress of side span are relatively small, the maximum tensile stress is 4MPa, and the maximum compressive stress is 13MPa. In addition, the maximum stress of the top plate is located at the end of the flange of the box section, which is not in the effective width area of the top plate for design. If the effective width for design of the top plate is considered, the stress value may degrease 1/3-1/2 times.

Due to the consolidation of piers and girder of continuous rigid frame bridges, the main girder also take part in the resistance some extent of seismic actions, but the main girder design does not consider the seismic load usually. According to the analysis of the construction process of the bridge and the continued time history analysis of the response of the box girder, it is found that the cracking design stress is 1.96MPa, and the initial stress of the top plate in the mid-span is about 6MPa(compression). Taken 051MZQ record as an example, the tensile stress of the top plate developed in the earthquake is more than 10MPa. It is estimated that when the PGA of the ground motion reaches 0.3g in the strong earthquake, the top plate will begin to crack. In the same way, it is calculated that the top plate of the girder's section for side span and web for mid-span, the plate may begin to crack when the PGA of the ground motion reaches 0.4g during strong earthquake. The section web for side span and section bottom plate of mid-span begin to crack when the PGA of the ground motion reaches 0.5g during strong earthquake. The section bottom plate for side span begin to crack when the PGA reaches 0.6g.

5. Estimation of Stress Increments of Pre-stressing Tendons

After the pre-stressing tendons being tensioned the pre-stressing pipelines were grouted with micro-expansion concrete to make the pre-stressing tendons and concrete tightly bonded in the process of construction. It is assumed that the strain increment of tendons and the strain increment of concretes is approximately the same during the earthquake.

$$\left.\begin{aligned} &\Delta\varepsilon_c \approx \Delta\varepsilon_s \\ &\Delta\sigma_c = \Delta\varepsilon_c \cdot E_c \\ &\Delta\sigma_s = \Delta\varepsilon_s \cdot E_s \end{aligned}\right\} \triangle\sigma_s = \left(E_s / E_c\right) \cdot \triangle\sigma_c \qquad (2)$$

where, E_c and E_s are the elastic modules of the steel and the concrete. It is concluded that the stress increment $\Delta\sigma_s$ of pre-stressing tendons is 5.42 times of that $\Delta\sigma_c$ of concrete at the same position of the box section.

According to the previous discussion, it is found that the maximum tensile stress increment of concrete for section's top plate appears near the mid-span. The maximum increment of stress for concrete is 18.7MPa, so the maximum stress increment of pre-stressing tendons is calculated to be about 100MPa. The initial effective tensile stress of the pre-stressing tendons of the top plate is 1200MPa, which will increase to 1300MPa under the combined effects of the initial load and seismic force, about 70% of the standard value f_{pk} (1860MPa) of the tensile strength of the pre-stressing tendons. The pre-stressing tendons' stress increment of section's bottom plate of side span and mid-span can reach 60MPa, and the maximum tensile stress can reach 1260MPa, which is about 67% of the standard value of tensile strength, indicating that pre-stressing tendons still has certain safety under the earthquake.

According to bridge design code JTG 3362-2018 in China [26], the maximum tensile stress of the pre-stressing tendons should be less than $0.65f_{pk}$ for bridge operation, that is 1209MPa. And the maximum tensile stress of pre-stressing tendons exceeds 7.5% of the specified value under the combined action of the dead load and earthquake load.

Cracks of the main girder were sealed with potting glue, and the bottom plate of the section at bridge mid-span was strengthened by pasting steel plate after Wenchuan earthquake. The stress change and loss of pre-stressing tendons under the earthquake were not considered during the repair work. After one year's operation of the bridge, it was found that some of the repaired web cracks cracked again, and the average deflection of mid-span section was 3cm [27]. As for the loss of prestress for tendons during earthquake, further research should be done. The research in this paper approximately gives the increment of stress for pre-stressing tendons.

6. Conclusion

In view of the girder's cracking damage of Miaoziping Bridge in Wenchuan earthquake, the numerical simulation of the seismic response of the main girder is carried out considering the initial stress of the box girder. The main findings are summarized as follows:

(1) results of numerical simulation are variety due to the influence of seismic input and other factors. However, the calculated high stress distribute areas of box girder's section are in good agreement with the real seismic damage of the bridge girder. To some extent, it indicates that the box girder's cracking seismic damage is not an individual phenomenon.

(2) box girder's numerical simulation results of Miaoziping Bridge display that the high（principle）tensile stress makes the main girder to crack easily. The high tensile stress areas of the sections include the web near 1/6 to 1/2 length of side span and the middle span length of 1/4 to 3/4, the bottom plate near the closure sections during the construction process and their adjacent 2-3 sections of the side span and the middle span, and the top plate near the closure section and its adjacent 2-3 sections of the middle span.

(3) under seismic actions, the stress of the longitudinal prestressed tendons increases to nearly 100 MPa near the middle span of the bridge.

7. Acknowledgements

In this paper, the girder's crack map of Miaoziping Bridge is mainly based on the reference [12], and thanks for their hard works in the filed investigation and later data publication. Professor Zhuang Weilin has provided the design drawings of the Miaoziping Bridge, and also thanks him here.

8. References

[1] Sun Z, Wang D, Wang T (2019): Investigation on seismic behavior of bridge piers with thin-walled rectangular hollow section using quasi-static cyclic tests, *Engineering Structures*, 200: 109708.

[2] Yang W, Li Q (2013): The expanded Morison equation considering inner and outer water hydrodynamic pressure of hollow piers, *Ocean Engineering*, 69: 79-87.

[3] Gu Y, Huang Y Zhou W (2011): Study on seismic vulnerability of long-span continuous rigid frame bridge with high piers, *Earthquake Engineering and Engineering Dynamics*, 31(02):91-97.

[4] Liu G, Feng X, Jiang D (2019): Failure Mode of Bridges Under Multi-support Excitation in a V-shaped Canyon with Multi-layer Topography, *China Journal of Highway and Transport*, 32(8): 101-113.

[5] Zhou G, Li X, Qi X (2010): Seismic response analysis of continuous rigid frame bridge considering canyon topography effects under incident SV waves, *Earthquake Science*, 23(1): 53-61.

[6] Jia H, Zhang D, Zheng S (2013): Local site effects on a high-pier railway bridge under tridirectional spatial excitations: nonstationary stochastic analysis, *Soil Dynamics and Earthquake Engineering*, 52:55-69.

[7] Li X, Li Z, Crewe A J (2018): Nonlinear seismic analysis of a high-pier, long-span, continuous RC frame bridge under spatially variable ground motions, *Soil Dynamics and Earthquake Engineering*, 114: 298-312.

[8] Yan X, Li Z, Han Q (2013): Shake tables test study on seismic response of a long-span rigid-framed bridge under multi-support excitations, *China Civil Engineering Journal*, 46(7): 81-89.

[9] Zong Z, Xia Z, Liu H (2016): Collapse failure of prestressed concrete continuous rigid-frame bridge under strong earthquake excitation: Testing and simulation, *Journal of Bridge Engineering*, 21(9): 04016047.

[10] Ministry of Transport of the People's Republic of China, (2008): Guidelines for seismic design of highway bridges. JTG/T B02-01-2008.

[11] Kawashima K, Takahashi Y, Ge H (2009): Reconnaissance report on damage of bridges in 2008 Wenchuan, China, earthquake[J]. *Journal of earthquake Engineering*, 13(7): 965-996.

[12] Chen L, Zhuang W, Zhao H (2012): The investigation of seismic bridge damage in the Wenchuan Earthquake, China Communication Press, 135-152.

[13] Xia Z (2003): Seismic response analysis of long span continuous rigid frame bridge. (MA. Eng Dissertation) Southwest Jiaotong University, P.R.China.

[14] YAO H (2003): Structural design special and features of Miaoziping Bridge, Southwest Highway, 2003(1):31-33.

[15] Wang D, GUO X, Sun Z (2009): Damage to highway bridges during Wenchuan Earthquake, *Journal of Earthquake Engineering and Engineering Vibration*, 29(03): 84-94.

[16] Wang D, Sun Z, Guo X (2011): Lessons learned from Wenchuan seismic damages and recent research on seismic design of highway bridges, *Journal of Highway and Transportation Research and Development*, 28(10): 44-53.

[17] Shan D, Zhang E, Dong J (2017): Ground motion attenuation characteristics of Wenchuan earthquake and seismic response law of long-span continuous rigid frame bridge with high-rise pier, *China Civil Engineering Journal*, (04):111-119.

[18] Chen F, Gu X, Shan D (2018): Seismic fragility analysis of irregular continuous rigid frame girder bridge, *Cogent Engineering*, 5(1): 1545741.

[19] Deng Y, Guo Q, Xu L (2019): Effects of Pounding and Fluid–Structure Interaction on Seismic Response of Long-Span Deep-Water Bridge with High Hollow Piers, *Arabian Journal for Science and Engineering*, 44(5): 4453-4465.

[20] Yang W, Li Q, Zhao C (2012): Failure mechanism analysis of main bridge of Miaoziping Bridge and seismic design measures, Harbin, P.R. China.

[21] Pan Z, You F. Quantitative design of backup prestressing tendons for long-span prestressed concrete box girder bridges(ASCE) [J]. *Journal of Bridge Engineering*, 2014, 20(3): 04014066.

[22] Huang H, Huang S , Pilakoutas K. Modeling for assessment of long-term behavior of prestressed concrete box-girder bridges (ASCE) [J]. *Journal of Bridge Engineering*, 2018, 23(3): 04018002.

[23] MA D (2008): Research on Construction Control of Long Span Continuous Rigid Frame Bridge. (MA.Eng Dissertation) Southwest Jiaotong University, P.R. China.

[24] Wang H (2016): Experimental Research on Seismic Behavior of Continuous Rigid Frame Concrete Bridge with High Pier and Long Span. (Ph.D. Dissertation) Northeast Forestry University, P.R. China.

[25] Kong X, Zhou Y, Zou D (2012): Study of seismic wave input of Zipingpu concrete face rockfill dam during Wenchuan earthquake, *Rock and Soil Mechanics*, 33(7):2110-2116.

[26] Ministry of Transport of the People's Republic of China, (2018): Specifcations for design of highway reinforced concrete and prestressed concrete bridges and culverts. JTG 3362–2018.

[27] Zhong E, Qin X (2012): Special Inspection for Structual Conditions of Minjiang Super large Bridge at Miaoziping on Duying Expressway, *Technology of Highway and Transport*, (6):75-79.

